Stanford Exploration Project, Report 117, October 23, 2004, pages 11–27

Stanford Exploration Project, Report 117, October 23, 2004, pages 11–27

High-order kernels for Riemannian wavefield extrapolation

Paul Sava[1]

ABSTRACT

High-order kernels for Riemannian wavefield extrapolation (RWE) are developed and demonstrated by impulse responses for models which are difficult or impossible to handle with Cartesian downward continuation. Those kernels improve the accuracy of extrapolation, particularly for situations when the Riemannian coordinate systems does not match closely the general direction of wave propagation (e.g. triplicating wavefields and migration from topography).

INTRODUCTION

Riemannian wavefield extrapolation (Sava and Fomel, 2003) generalizes solutions to the Helmholtz equation in general Riemannian coordinate systems. The main requirements imposed on the Riemannian coordinate systems are that they maintain orthogonality between the extrapolation coordinate and the other coordinates (2 in 3D, 1 in 2D). In addition, it is desirable that the coordinate system does not triplicate, although numerical methods can stabilize extrapolation even in such situations. Thus, wavefield extrapolation in Riemannian coordinates has the flexibility to be used in many applications where those basic conditions are fulfilled. Cartesian coordinate systems, including tilted coordinates, are special cases of Riemannian coordinate systems. Two straightforward examples of wave propagation in Riemannian coordinates are extrapolation in a coordinate system created by ray tracing in a smooth background velocity (Sava and Fomel, 2003), and extrapolation with a coordinate system created by conformally mapping a given geometry to a regular space, for example migration from topography (Shragge and Sava, 2004).

Coordinate systems created by ray tracing in a background medium often well represent wavefield propagation. In this context, we effectively split wave propagation effects into two parts: one part accounting for the general trend of wave propagation, which is incorporated in the coordinate system, and the other part accounting for the details of wavefield scattering due to rapid velocity variations. If the background medium is close to the real one, the wave-propagation can be properly described with low-order operators. However, if the background medium is far from the true one, the wavefield departs from the general direction of the coordinate system and the low-order extrapolators are not enough for accurate description of wave propagation.

[1]**email:** paul@sep.stanford.edu

For coordinate system describing a geometrical property of the medium (e.g. migration from topography), there is no guarantee that waves propagate in the direction of extrapolation. This situation is similar to that of Cartesian coordinates when waves propagate away from the vertical direction, except that conformal mapping gives us the flexibility to define any coordinates, as required by acquisition. In this case, too, low-order extrapolators are not enough for accurate description of wave propagation.

Therefore, we need to develop higher-order Riemannian wavefield extrapolators in order to handle correctly waves propagating obliquely with the coordinate system. Usually, the high-order extrapolators are implemented as mixed operators, part in the Fourier domain using a reference medium, part in the space domain as a correction from the reference medium. Many methods have been developed for high-order extrapolation in Cartesian coordinates. In this paper, I explore some of those extrapolators in Riemannian coordinates. In particular, I concentrate on high-order finite-differences solutions, and methods from the pseudo-screen family (Huang et al., 1999) and Fourier finite-differences family (Ristow and Ruhl, 1994; Biondi, 2002). In theory, any other high-order extrapolator developed in Cartesian coordinates can have a correspondent in Riemannian coordinates.

In this paper, I implement the finite-differences portion of the high-order extrapolators with implicit methods. Such solutions are accurate and robust, but they face difficulties for 3D implementations because the finite-differences part cannot be solved by fast tridiagonal solvers anymore and require more complex and costlier approaches (Fomel and Claerbout, 1997; Rickett et al., 1998). The problem of 3D wavefield extrapolation is addressed in Cartesian coordinates either by splitting the one-way wave-equation along orthogonal directions (Ristow and Ruhl, 1997), or by explicit numerical solutions (Hale, 1991). Similar approaches can be envisioned for 3D Riemannian extrapolation. The explicit solution seems more appropriate, since splitting is difficult due to the mixed terms of the Riemannian equations. I do not address this subject in this paper, and concentrate on developing higher-order kernels with implicit methods.

RIEMANNIAN WAVEFIELD EXTRAPOLATION

Riemannian wavefield extrapolation (Sava and Fomel, 2003) generalizes solutions to the Helmholtz equation

$$\Delta \mathcal{U} = -\omega^2 s^2 \mathcal{U} \,, \tag{1}$$

to coordinate systems that are different from simple Cartesian, where extrapolation is performed strictly in the downward direction. In equation (1), s is slowness, ω is temporal frequency, and $\mathcal{U}$ is a monochromatic wave.

The acoustic wave-equation in Riemannian coordinates can be written as:

$$c_{\zeta\zeta}\frac{\partial^2 \mathcal{U}}{\partial \zeta^2}+c_{\xi\xi}\frac{\partial^2 \mathcal{U}}{\partial \xi^2}+c_{\eta\eta}\frac{\partial^2 \mathcal{U}}{\partial \eta^2}+c_{\zeta}\frac{\partial \mathcal{U}}{\partial \zeta}+c_{\xi}\frac{\partial \mathcal{U}}{\partial \xi}+c_{\eta}\frac{\partial \mathcal{U}}{\partial \eta}+c_{\xi\eta}\frac{\partial^2 \mathcal{U}}{\partial \xi \partial \eta} = -(\omega s)^2 \mathcal{U} \,, \tag{2}$$

where coefficients c_{ij} are functions of the coordinate system and can be computed numerically for any given coordinate system (Sava and Fomel, 2003).

We can simplify the Riemannian wavefield extrapolation method by dropping the first-order terms in equation (2). According to the theory of characteristics for second-order hyperbolic equations (Courant and Hilbert, 1989), these terms affect only the amplitude of the propagating waves. To preserve the kinematics, it is sufficient to keep only the second order terms of equation (2):

$$c_{\zeta\zeta}\frac{\partial^2 \mathcal{U}}{\partial \zeta^2}+c_{\xi\xi}\frac{\partial^2 \mathcal{U}}{\partial \xi^2}+c_{\eta\eta}\frac{\partial^2 \mathcal{U}}{\partial \eta^2}+c_{\xi\eta}\frac{\partial^2 \mathcal{U}}{\partial \xi\,\partial \eta}=-\left(\omega s\right)^2\mathcal{U}\,. \tag{3}$$

From equation (3) we can derive the following dispersion relation:

$$-c_{\zeta\zeta}k_\zeta^2-c_{\xi\xi}k_\xi^2-c_{\eta\eta}k_\eta^2-c_{\xi\eta}k_\xi k_\eta=-\left(\omega s\right)^2\,, \tag{4}$$

where k_ζ, k_ξ and k_η are wavenumbers associated with the Riemannian coordinates ζ, ξ and η.

For one-way wavefield extrapolation, we need to solve the quadratic equation (4) for the wavenumber of the extrapolation direction k_ζ, and select the solution with the appropriate sign to extrapolate waves in the desired direction:

$$k_\zeta=\sqrt{\frac{\left(\omega s\right)^2}{c_{\zeta\zeta}}-\frac{c_{\xi\xi}}{c_{\zeta\zeta}}k_\xi^2-\frac{c_{\eta\eta}}{c_{\zeta\zeta}}k_\eta^2-\frac{c_{\xi\eta}}{c_{\zeta\zeta}}k_\xi k_\eta}\,. \tag{5}$$

The 2D equivalent of equation (5) takes the form:

$$k_\zeta=\sqrt{\frac{\left(\omega s\right)^2}{c_{\zeta\zeta}}-\frac{c_{\xi\xi}}{c_{\zeta\zeta}}k_\xi^2}\,. \tag{6}$$

In ray coordinates, defined by $\zeta\equiv\tau$ and $\xi\equiv\gamma$, we can re-write equation (6) as

$$k_\tau=\sqrt{\left(\omega s\alpha\right)^2-\left(\frac{\alpha}{J}k_\gamma\right)^2}\,, \tag{7}$$

where α is velocity and J is geometrical spreading. We can simplify the computations by the notation

$$\left\{\begin{array}{l} a=s\alpha\,,\\ b=\frac{\alpha}{J}\,,\end{array}\right. \tag{8}$$

therefore, equation (7) takes the form

$$k_\tau=\sqrt{\left(\omega a\right)^2-\left(bk_\gamma\right)^2}\,. \tag{9}$$

THEORY

Space-domain solution

The space-domain finite-differences solution to equation (9) is derived based on the square-root expansion, first introduced to Geophysics by Muir (Claerbout, 1985):

$$k_\tau \approx \omega a + \omega \frac{\nu \left(\frac{k_\gamma}{\omega}\right)^2}{\mu - \rho \left(\frac{k_\gamma}{\omega}\right)^2} , \tag{10}$$

where the coefficients μ, ν and ρ take the form:

$$\begin{cases} \nu = -c_1 a \left(\frac{b}{a}\right)^2 , \\ \mu = 1 , \\ \rho = c_2 \left(\frac{b}{a}\right)^2 . \end{cases} \tag{11}$$

In the special case of Cartesian coordinates, $a = s$ and $b = 1$, equation (10) takes the familiar form

$$k_\tau \approx \omega s - \omega \frac{\frac{c_1}{s} \left(\frac{k_\gamma}{\omega}\right)^2}{1 - \frac{c_2}{s^2} \left(\frac{k_\gamma}{\omega}\right)^2} , \tag{12}$$

where the coefficients c_1 and c_2 take different values for different orders of the Muir expansion: $c_{15} = (c_1, c_2) = (0.50, 0.00)$ for the 15° equation, and $c_{45} = (c_1, c_2) = (0.50, 0.25)$ for the 45° equation.

Mixed-domain solutions

Mixed-domain solutions to the one-way wave equation usually consist of terms computed in the Fourier domain for a reference of the extrapolation medium, followed by a finite-differences correction applied in the space-domain. For equation (9), a generic mixed-domain solution has the form:

$$k_\tau \approx k_{\tau 0} + \omega (a - a_0) + \omega \frac{\nu \left(\frac{k_\gamma}{\omega}\right)^2}{\mu - \rho \left(\frac{k_\gamma}{\omega}\right)^2} , \tag{13}$$

where a_0 and b_0 are reference values for the medium characterized by the parameters a and b, and the coefficients μ, ν and ρ take different forms according to the type of approximation. As for usual Cartesian coordinates, $k_{\tau 0}$ is applied in the Fourier domain, and the other two terms are applied in the space domain. If we limit the space-domain correction to the thin lens term, $\omega(a - a_0)$, we obtain the equivalent of split-step Fourier (SSF) method (Stoffa et al., 1990) in Riemannian coordinates.

Appendix A details the derivations for two types of expansions: pseudo-screen (Huang et al., 1999), and Fourier finite-differences (Ristow and Ruhl, 1994; Biondi, 2002).

- **Pseudo-screen:**

  The coefficients for the pseudo-screen solution to equation (13) are

$$\left\{ \begin{array}{l} \nu = a_0 \left[c_1 \left(\frac{a}{a_0} - 1 \right) - \left(\frac{b}{b_0} - 1 \right) \right] \left(\frac{b_0}{a_0} \right)^2 , \\ \mu = 1 , \\ \rho = 3 c_2 \left(\frac{b_0}{a_0} \right)^2 , \end{array} \right. \tag{14}$$

  where a_0 and b_0 are reference values for the medium characterized by parameters a and b. In the special case of Cartesian coordinates, $a = s$ and $b = 1$, equation (13) with coefficients equation (14) takes the familiar form

$$k_\tau \approx k_{\tau 0} + \omega \left[1 + \frac{\frac{c_1}{s_0^2} \left(\frac{k_\gamma}{\omega} \right)^2}{1 - \frac{3c_2}{s_0^2} \left(\frac{k_\gamma}{\omega} \right)^2} \right] (s - s_0) , \tag{15}$$

  where the coefficients c_1 and c_2 take different values for different orders of the finite-differences term: $c_{15} = (c_1, c_2) = (0.50, 0.00)$ and $c_{45} = (c_1, c_2) = (0.50, 0.25)$. When $(c_1, c_2) = (0.00, 0.00)$ we obtain the usual split-step Fourier equation.

- **Fourier finite-differences:**

  The coefficients for the Fourier finite-differences solution to equation (13) are

$$\left\{ \begin{array}{l} \nu = \frac{1}{2} \delta_1^2 , \\ \mu = \delta_1 , \\ \rho = \frac{1}{4} \delta_2 , \end{array} \right. \tag{16}$$

  where

$$\left\{ \begin{array}{l} \delta_1 = a \left(\frac{b}{a} \right)^2 - a_0 \left(\frac{b_0}{a_0} \right)^2 , \\ \delta_2 = a \left(\frac{b}{a} \right)^4 - a_0 \left(\frac{b_0}{a_0} \right)^4 . \end{array} \right. \tag{17}$$

  a_0 and b_0 are reference values for the medium characterized by the parameters a and b. In the special case of Cartesian coordinates, $a = s$ and $b = 1$, equation (13) with coefficients equation (16) takes the familiar form:

$$k_\tau \approx k_{\tau 0} + \omega \left[1 + \frac{\frac{c_1}{s s_0} \left(\frac{k_\gamma}{\omega} \right)^2}{1 - c_2 \left(\frac{1}{s^2} + \frac{1}{s s_0} + \frac{1}{s_0^2} \right) \left(\frac{k_\gamma}{\omega} \right)^2} \right] (s - s_0) , \tag{18}$$

  where the coefficients c_1 and c_2 take different values for different orders of the finite-differences term: $c_1 = 0.5, c_2 = 0.0$ for 15°, or $c_1 = 0.5, c_2 = 0.25$ for 45°. When $c_1 = c_2 = 0.0$ we obtain the usual split-step Fourier equation.

EXAMPLES

I illustrate the higher-order RWE extrapolators with impulse responses for two models with increasing levels of complexity.

The first example is based on a model with two smooth velocity anomalies that generate focusing and defocussing of the coordinate system, without triplication. I construct the coordinate system by ray tracing from an incident horizontal plane-wave at the surface. Figure 1 shows the velocity model with the coordinate system overlayed. Figure 2 shows the coordinate system coefficients defined in equation (9).

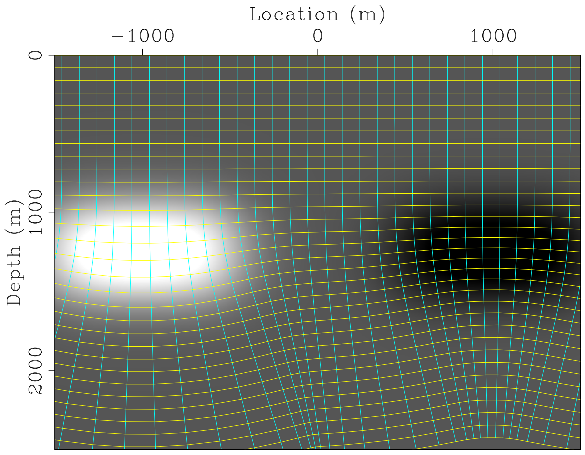

Figure 1: Velocity map and Riemannian coordinate system. paul1-RWEimp0.cos [CR]

The goal of this test model is to illustrate the higher-order extrapolation kernels in a fairly simple coordinate system which is close to a Cartesian basis. The coordinate system is constructed from an incident plane wave, while the data comes from a point source. This setting is almost identical to the case of extrapolation from a point source in Cartesian coordinates, where high-angle [2] propagation requires high-order kernels. In this case, the Riemannian coordinate system does not match closely the general direction of wave propagation, so higher order kernels are needed. In practice, this situation can be addressed better with synthesized plane-wave data extrapolated in a coordinate system ray traced from an incident plane, and with point source data extrapolated in a coordinate system ray traced from a point source.

Figure 3 shows the velocity model and impulse responses for a point source computed with various extrapolators in ray coordinates (τ and γ). Panel (a) shows the slowness model, panel (b) shows extrapolation with the 15° finite-differences equation, panel (c) shows extrapolation with the 45° finite-differences equation, panel (d) shows extrapolation with the split-step Fourier (SSF) equation, panel (e) shows extrapolation with the pseudo-screen (PSC) equation, and panel (f) shows extrapolation with the Fourier finite-differences (FFD) equation. All plots are displayed in ray coordinates. We can observe that the angular accuracy of the extrapolator improves for the more accurate extrapolators. The finite-differences solutions (panels b and c)

[2]If the extrapolation axis is time, the meaning of higher angle accuracy is not well defined. We can use this terminology to associate the mathematical meaning of the approximation for the square-root by analogy with the Cartesian equivalents.

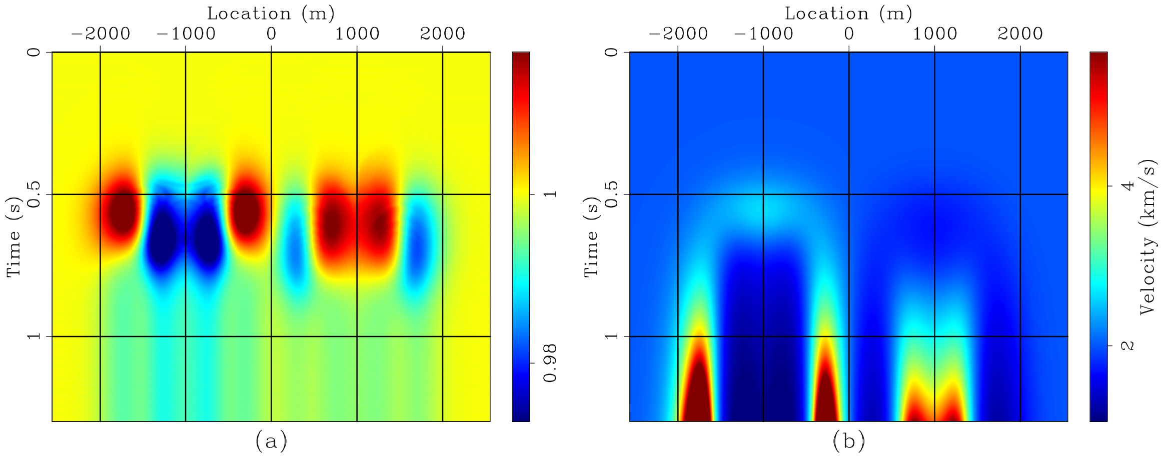

Figure 2: (a) Parameter $a = s\alpha$ in ray coordinates. (b) Parameter $b = \alpha / J$ in ray coordinates. paul1-RWEimp0.ab [CR,M]

show the typical behavior of such solutions for the 15° and 45° equations (e.g. the cardioid for 45°), but in the more general setting of Riemannian extrapolation. The mixed-domain extrapolators (panels d, e, and f) show increased accuracy. The main differences occur at the highest propagation angles, and the most accurate extrapolators of those compared is the equivalent of Fourier finite-differences (panel f).

Figure 4 shows the corresponding plots in Figure 3 mapped in the physical coordinates, except for panel (a) which in this case shows the impulse response for extrapolation in Cartesian coordinates using a Fourier finite-differences extrapolator with a 15° finite-differences term. The overlay is an outline of the extrapolation coordinate system. After re-mapping to the physical space, the comparison of high-angle accuracy for the various extrapolators is more obvious, since it now has the proper physical meaning.

The second example is based on a model with a large lateral gradient which makes an incident plane wave overturn. A small Gaussian anomaly forces the coordinate system to focus slightly, and another large Gaussian anomaly, not used for the coordinate system, forces the propagating wave to triplicate and move at high angles relative to the extrapolation direction. Figure 5 shows the velocity model with the coordinate system overlayed. Figure 6 shows the coordinate system coefficients defined in equation (9).

The goal of this model is to illustrate Riemannian wavefield extrapolation in a situation which cannot be handled correctly by Cartesian extrapolation, no matter how accurate. In this example, an incident plane wave is overturning, thus becoming evanescent for the solution in Cartesian coordinates. Furthermore, the large Gaussian anomaly, Figure 6(a), causes serious wavefield triplication, thus requiring high-order kernels in the Riemannian extrapolator.

Figure 7 shows the velocity model and impulse responses for an incident plane wave computed with various extrapolators in ray coordinates (τ and γ). Panel (a) shows the slowness model, panel (b) shows extrapolation with the 15° finite-differences equation, panel (c) shows extrapolation with the 45° finite-differences equation, panel (d) shows extrapolation with the

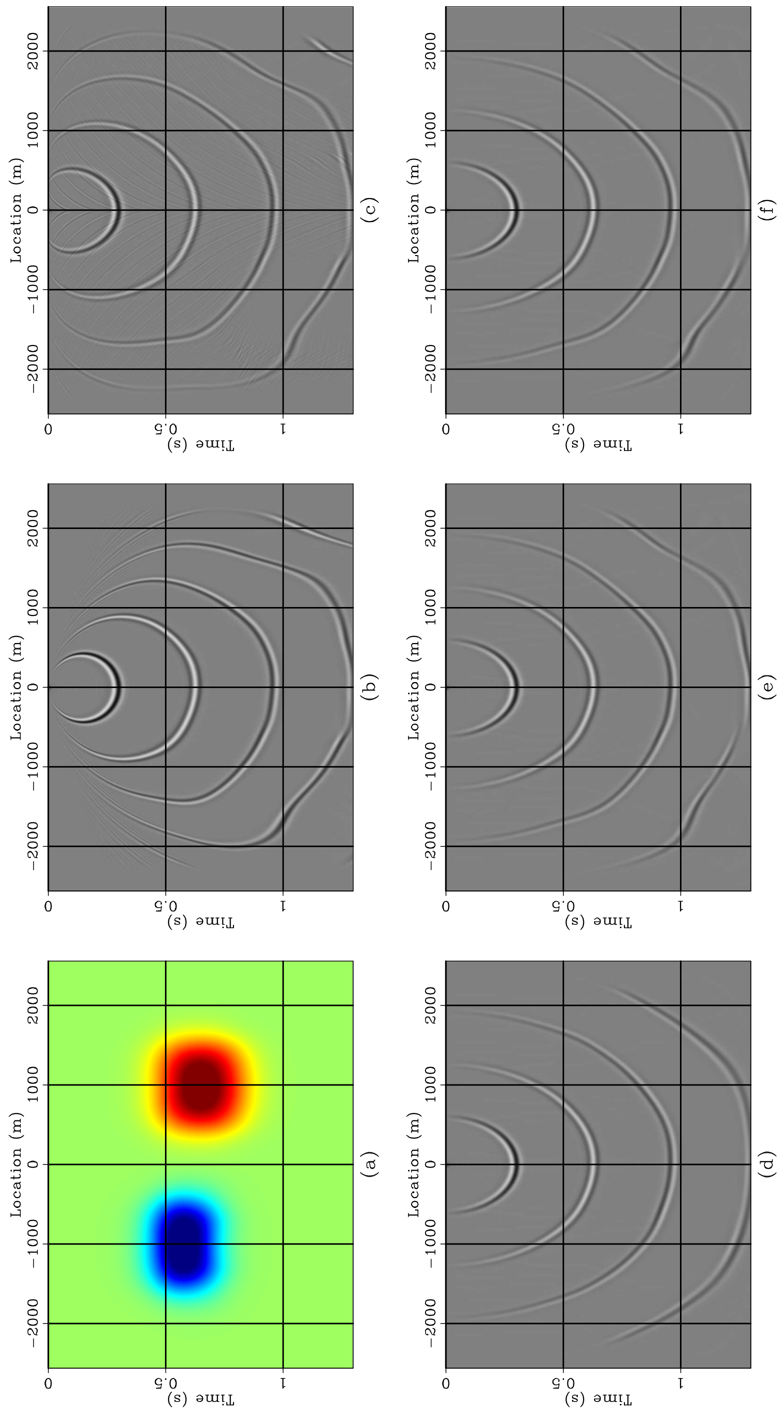

Figure 3: (a) Slowness. (b) Extrapolation with the 15° finite-differences equation. (c) Extrapolation with the 45° finite-differences equation. (d) Extrapolation with the split-step Fourier (SSF) equation. (e) Extrapolation with the pseudo-screen (PSC) equation. (f) Extrapolation with the Fourier finite-differences (FFD) equation. paul1-RWEimp0.rweimg [CR,M]

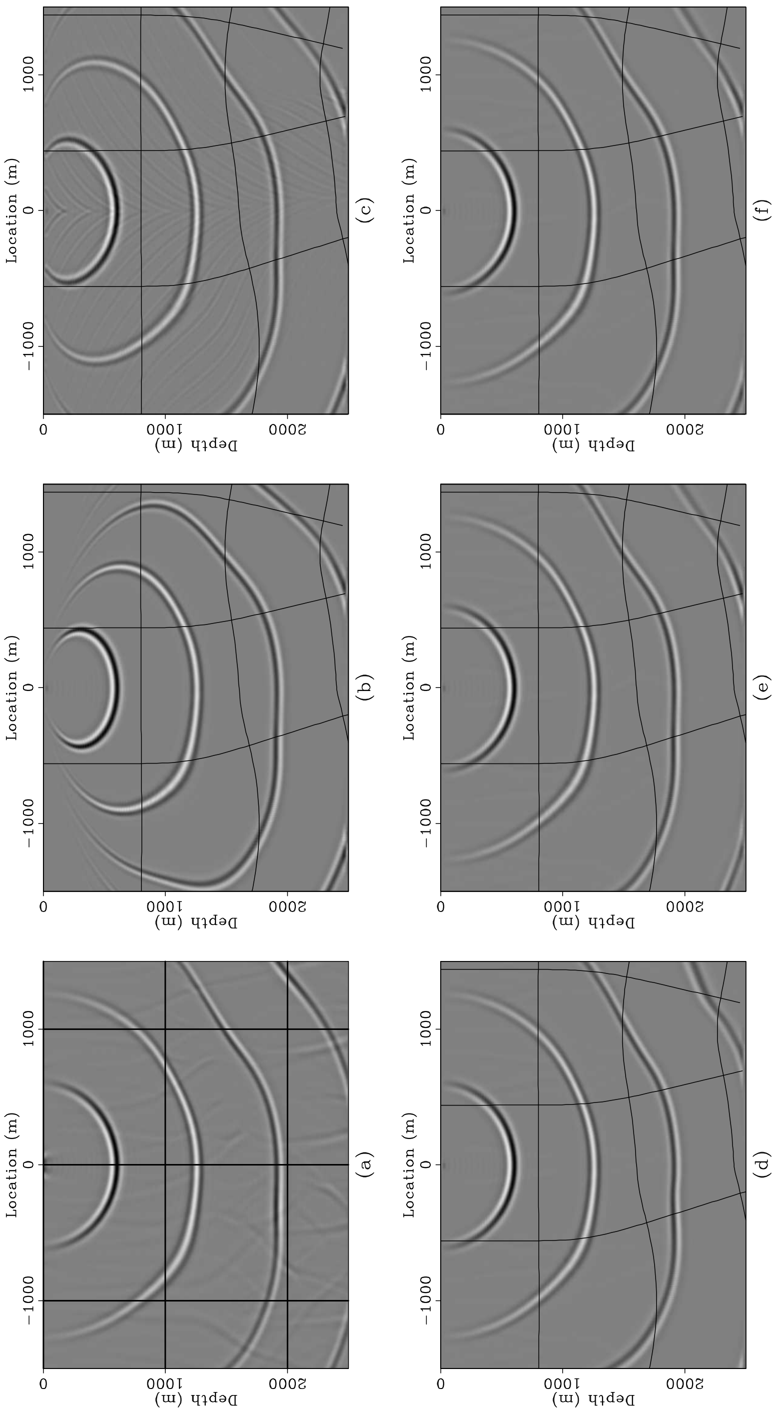

Figure 4: (a) Extrapolation with the Fourier finite-differences (FFD) equation in Cartesian coordinates. (b) Extrapolation with the 15° finite-differences equation. (c) Extrapolation with the 45° finite-differences equation. (d) Extrapolation with the split-step Fourier (SSF) equation. (e) Extrapolation with the pseudo-screen (PSC) equation. (f) Extrapolation with the Fourier finite-differences (FFD) equation. paul1-RWEimp0.carimg [CR,M]

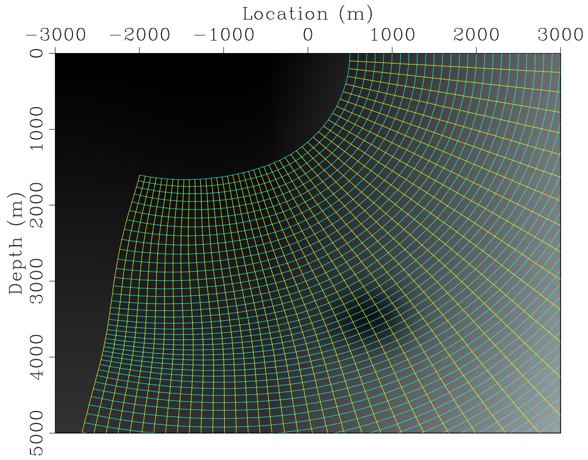

Figure 5: Velocity map and Riemannian coordinate system. paul1-RWEimp1.cos [CR]

split-step Fourier (SSF) equation, panel (e) shows extrapolation with the pseudo-screen (PSC) equation, and panel (f) shows extrapolation with the Fourier finite-differences (FFD) equation. All plots are displayed in ray coordinates. As with the preceding example, we can observe increased angular accuracy as we increase the order of the extrapolator. The equivalent FFD is the most accurate.

As in the preceding example, Figure 4 shows the corresponding plots in Figure 3 mapped in the physical coordinates, except for panel (a) which in this case shows the impulse response for extrapolation in Cartesian coordinates using a Fourier finite-differences extrapolator with a 15° finite-differences term. The overlay is an outline of the extrapolation coordinate system.

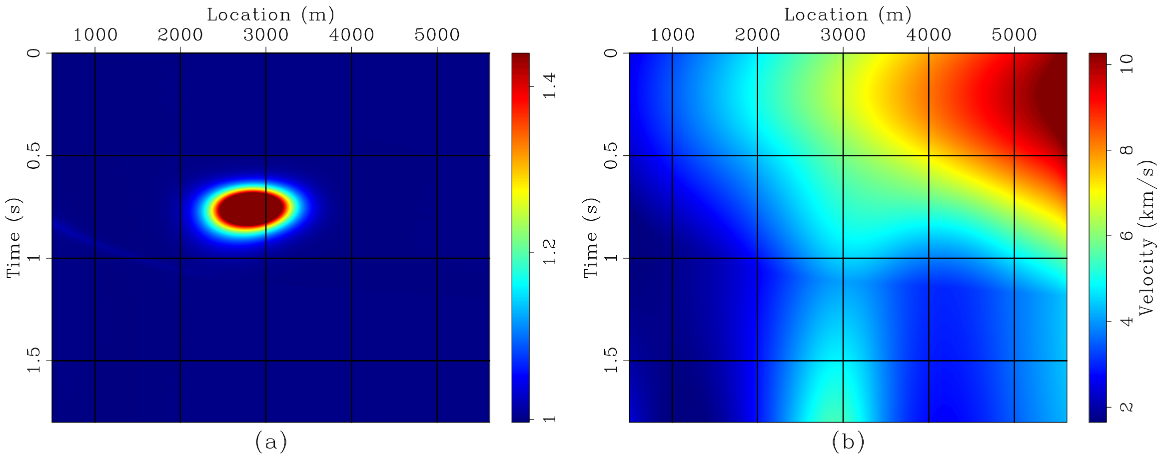

Figure 6: (a) Parameter $a = s\alpha$ in ray coordinates. (b) Parameter $b = \alpha/J$ in ray coordinates. paul1-RWEimp1.ab [CR,M]

Panel (a) in Figure 8 clearly shows the failure of the Cartesian extrapolator in propagating waves correctly even up to 90°. All Riemannian extrapolators handle better the overturning waves, including energy that is propagating upward relative to the physical coordinates. As expected, the higher order kernels are more accurate in describing the triplicating wavefields.

CONCLUSIONS

Higher-order Riemannian wavefield extrapolation is needed when the coordinate system does not closely conform with the general direction of wavefield propagation. This situation occurs, for example, when the coordinate system is created by ray tracing in a medium that is different from the one used for extrapolation, or when the coordinate system is constructed based on some geometrical properties of the acquisition geometry (e.g. migration from topography). Space-domain and mixed-domain finite-difference solutions to Riemannian wavefield extrapolation improve the angular accuracy. 3D solutions can be addressed with explicit finite-differences, although this remains subject for future research.

ACKNOWLEDGMENT

Sergey Fomel contributed to the initial development of the higher-order finite differences kernels for Riemannian wavefield extrapolation.

REFERENCES

Biondi, B., 2002, Stable wide-angle Fourier finite-difference downward extrapolation of 3-D wavefields: Geophysics, **67**, no. 03, 872–882.

Claerbout, J. F., 1985, Imaging the Earth's Interior: Blackwell Scientific Publications.

Courant, R., and Hilbert, D., 1989, Methods of mathematical physics: John Wiley & Sons.

Fomel, S., and Claerbout, J. F., 1997, Exploring three-dimensional implicit wavefield extrapolation with the helix transform: SEP–**95**, 43–60.

Hale, D., 1991, Stable explicit depth extrapolation of seismic wavefields: Geophysics, **56**, no. 11, 1770–1777.

Huang, L. Y., Fehler, M. C., and Wu, R. S., 1999, Extended local Born Fourier migration method: Geophysics, **64**, no. 5, 1524–1534.

Rickett, J., Claerbout, J., and Fomel, S., 1998, Implicit 3-D depth migration by wavefield extrapolation with helical boundary conditions: SEP–**97**, 1–12.

Ristow, D., and Ruhl, T., 1994, Fourier finite-difference migration: Geophysics, **59**, no. 12, 1882–1893.

Ristow, D., and Ruhl, T., 1997, 3-D implicit finite-difference migration by multiway splitting: Geophysics, **62**, no. 02, 554–567.

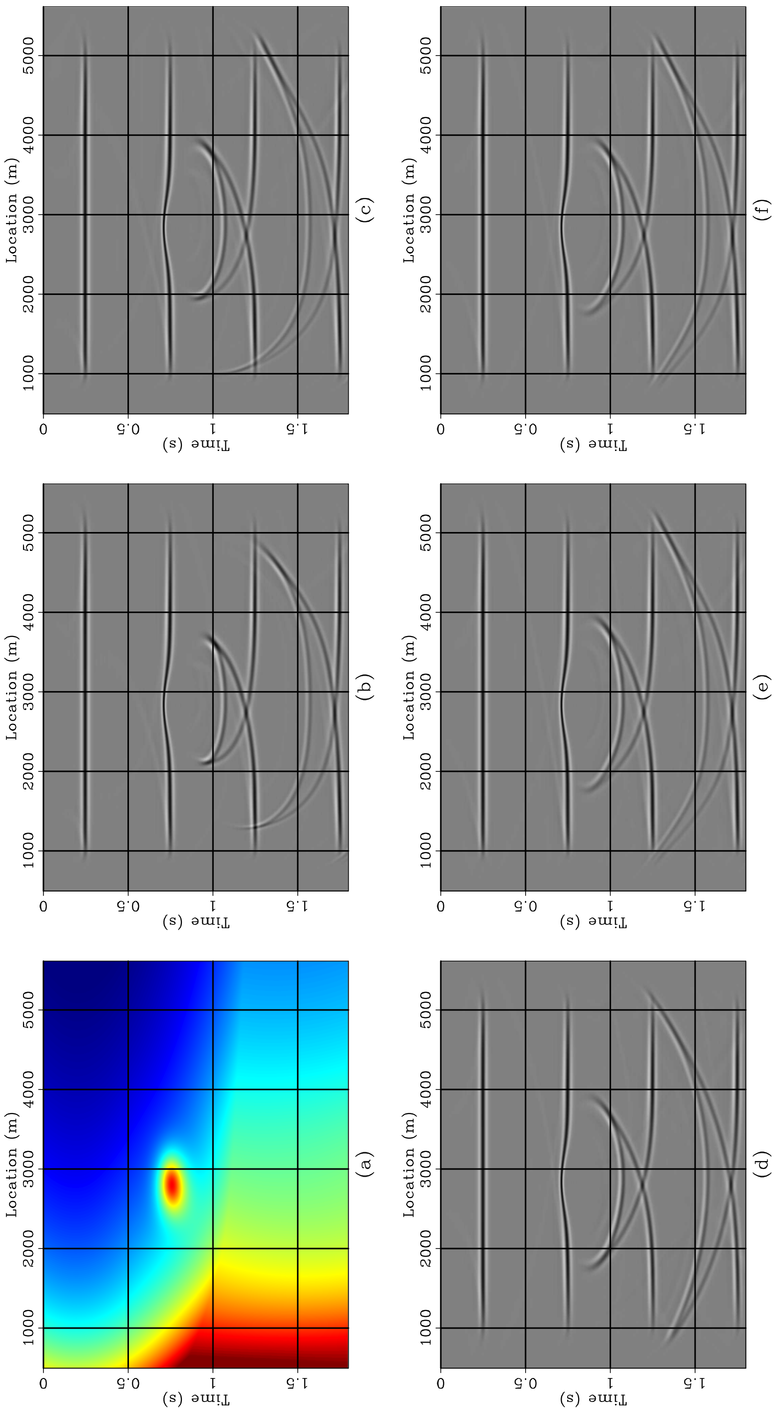

Figure 7: (a) Slowness. (b) Extrapolation with the 15° finite-differences equation. (c) Extrapolation with the 45° finite-differences equation. (d) Extrapolation with the split-step Fourier (SSF) equation. (e) Extrapolation with the pseudo-screen (PSC) equation. (f) Extrapolation with the Fourier finite-differences (FFD) equation. paul1-RWEimp1.rweimg [CR,M]

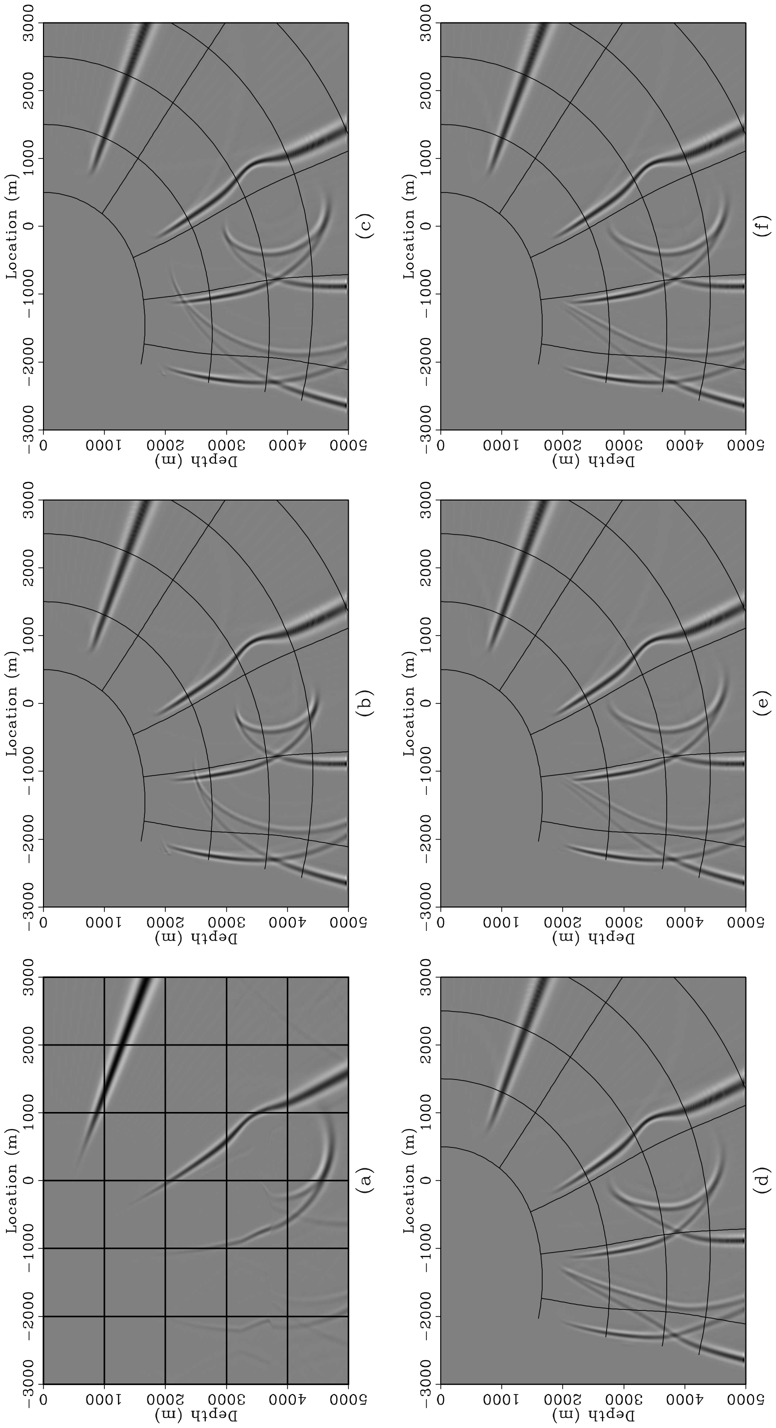

Figure 8: (a) Extrapolation with the Fourier finite-differences (FFD) equation in Cartesian coordinates. (b) Extrapolation with the 15° finite-differences equation. (c) Extrapolation with the 45° finite-differences equation. (d) Extrapolation with the split-step Fourier (SSF) equation. (e) Extrapolation with the pseudo-screen (PSC) equation. (f) Extrapolation with the Fourier finite-differences (FFD) equation. paul1-RWEimp1.carimg [CR,M]

Sava, P., and Fomel, S., 2003, Seismic imaging using Riemannian wavefield extrapolation: SEP–**114**, 1–30.

Shragge, J., and Sava, P., 2004, Incorporating topography into wave-equation imaging through conformal mapping: SEP–**117**.

Stoffa, P. L., Fokkema, J. T., de Luna Freire, R. M., and Kessinger, W. P., 1990, Split-step Fourier migration: Geophysics, **55**, no. 04, 410–421.

APPENDIX A

SPACE-DOMAIN FINITE-DIFFERENCES

Starting from equation (9), based on the Muir expansion for the square-root (Claerbout, 1985), we can write successively:

$$k_\tau = \omega a \sqrt{1-\left(\frac{bk_\gamma}{a\omega}\right)^2} \quad \text{(A-1)}$$

$$\approx \omega a \left[1-\frac{c_1\left(\frac{bk_\gamma}{a\omega}\right)^2}{1-c_2\left(\frac{bk_\gamma}{a\omega}\right)^2}\right] \quad \text{(A-2)}$$

$$\approx \omega a - \omega \frac{c_1 a\left(\frac{b}{a}\right)^2\left(\frac{k_\gamma}{\omega}\right)^2}{1-c_2\left(\frac{b}{a}\right)^2\left(\frac{k_\gamma}{\omega}\right)^2} . \quad \text{(A-3)}$$

If we make the notations

$$\begin{cases} \nu = -c_1 a\left(\frac{b}{a}\right)^2 , \\ \mu = 1 , \\ \rho = c_2\left(\frac{b}{a}\right)^2 . \end{cases} \quad \text{(A-4)}$$

we obtain the finite-differences solution to the one-way wave equation in Riemannian coordinates:

$$k_\tau \approx \omega a + \omega \frac{\nu\left(\frac{k_\gamma}{\omega}\right)^2}{\mu-\rho\left(\frac{k_\gamma}{\omega}\right)^2} . \quad \text{(A-5)}$$

MIXED DOMAIN — PSEUDO-SCREEN

The pseudo-screen solution to equation (9) derives from a first-order expansion of the square-root around a_0 and b_0 which are reference values for the medium characterized by the parameters a and b:

$$k_\tau \approx k_{\tau 0} + \left.\frac{\partial k_\tau}{\partial a}\right|_{a_0,b_0} (a-a_0) + \left.\frac{\partial k_\tau}{\partial b}\right|_{a_0,b_0} (b-b_0) \; . \tag{A-6}$$

The partial derivatives relative to a and b, respectively, are:

$$\left.\frac{\partial k_\tau}{\partial a}\right|_{a_0,b_0} = \omega \frac{1}{\sqrt{1-\left(\frac{b_0 k_\gamma}{a_0 \omega}\right)^2}} \approx \omega \left[1 + \frac{c_1 \left(\frac{b_0 k_\gamma}{a_0 \omega}\right)^2}{1 - 3c_2 \left(\frac{b_0 k_\gamma}{a_0 \omega}\right)^2} \right] , \tag{A-7}$$

$$\left.\frac{\partial k_\tau}{\partial b}\right|_{a_0,b_0} = -\omega \frac{b_0}{a_0} \left(\frac{k_\gamma}{\omega}\right)^2 \frac{1}{\sqrt{1-\left(\frac{b_0 k_\gamma}{a_0 \omega}\right)^2}} \approx -\omega \frac{a_0}{b_0} \left(\frac{b_0 k_\gamma}{a_0 \omega}\right)^2 . \tag{A-8}$$

Therefore, the pseudo-screen equation becomes

$$k_\tau \approx k_{\tau 0} + \omega (a-a_0) + \omega \frac{a_0 \left[c_1 \left(\frac{a}{a_0}-1\right) - \left(\frac{b}{b_0}-1\right)\right] \left(\frac{b_0}{a_0}\right)^2 \left(\frac{k_\gamma}{\omega}\right)^2}{1 - 3c_2 \left(\frac{b_0}{a_0}\right)^2 \left(\frac{k_\gamma}{\omega}\right)^2} . \tag{A-9}$$

If we make the notations

$$\left\{ \begin{array}{l} \nu = a_0 \left[c_1 \left(\frac{a}{a_0}-1\right) - \left(\frac{b}{b_0}-1\right)\right] \left(\frac{b_0}{a_0}\right)^2 \\ \mu = 1 \\ \rho = 3c_2 \left(\frac{b_0}{a_0}\right)^2 \end{array} \right. \tag{A-10}$$

we obtain the mixed-domain pseudo-screen solution to the one-way wave equation in Riemannian coordinates:

$$k_\tau \approx k_{\tau 0} + \omega (a-a_0) + \omega \frac{\nu \left(\frac{k_\gamma}{\omega}\right)^2}{\mu - \rho \left(\frac{k_\gamma}{\omega}\right)^2} . \tag{A-11}$$

MIXED DOMAIN — FOURIER FINITE-DIFFERENCES

The pseudo-screen solution to equation (9) derives from a fourth-order expansion of the square-root around (a_0, b_0) and (a, b):

$$k_\tau \approx \omega a \left[1 + \frac{1}{2} \left(\frac{b k_\gamma}{a \omega}\right)^2 + \frac{1}{8} \left(\frac{b k_\gamma}{a \omega}\right)^4 \right] ,$$

$$k_{\tau 0} \approx \omega a_0 \left[1 + \frac{1}{2} \left(\frac{b_0 k_\gamma}{a_0 \omega}\right)^2 + \frac{1}{8} \left(\frac{b_0 k_\gamma}{a_0 \omega}\right)^4 \right] . \tag{A-12}$$

If we subtract equations (A-12), we obtain:

$$k_\tau \approx k_{\tau 0} + \omega (a - a_0) + \frac{1}{2}\omega \left[a \left(\frac{b}{a}\right)^2 - a_0 \left(\frac{b_0}{a_0}\right)^2 \right] \left(\frac{k_\gamma}{\omega}\right)^2 + \frac{1}{8}\omega \left[a \left(\frac{b}{a}\right)^4 - a_0 \left(\frac{b_0}{a_0}\right)^4 \right] \left(\frac{k_\gamma}{\omega}\right)^4 . \tag{A-13}$$

We can make the notations

$$\delta_1 = a \left(\frac{b}{a}\right)^2 - a_0 \left(\frac{b_0}{a_0}\right)^2 , \tag{A-14}$$

$$\delta_2 = a \left(\frac{b}{a}\right)^4 - a_0 \left(\frac{b_0}{a_0}\right)^4 , \tag{A-15}$$

therefore equation (A-13) becomes

$$k_\tau = k_{\tau 0} + \omega (a - a_0) + \frac{1}{2}\omega \delta_1 \left(\frac{k_\gamma}{\omega}\right)^2 + \frac{1}{8}\omega \delta_2 \left(\frac{k_\gamma}{\omega}\right)^4 . \tag{A-16}$$

With the approximation

$$\frac{1}{2}\delta_1 u^2 + \frac{1}{8}\delta_2 u^4 \approx \frac{\frac{1}{2}\delta_1^2 u^2}{\delta_1 - \frac{1}{4}\delta_2 u^2} , \tag{A-17}$$

we can write

$$k_\tau = k_{\tau 0} + \omega (a - a_0) + \omega \frac{\frac{1}{2}\delta_1^2 \left(\frac{k_\gamma}{\omega}\right)^2}{\delta_1 - \frac{1}{4}\delta_2 \left(\frac{k_\gamma}{\omega}\right)^2} . \tag{A-18}$$

If we make the notations

$$\begin{cases} \nu = \frac{1}{2}\delta_1^2 , \\ \mu = \delta_1 , \\ \rho = \frac{1}{4}\delta_2 , \end{cases} \tag{A-19}$$

we obtain the mixed-domain Fourier finite-differences solution to the one-way wave equation in Riemannian coordinates:

$$k_\tau \approx k_{\tau 0} + \omega (a - a_0) + \omega \frac{\nu \left(\frac{k_\gamma}{\omega}\right)^2}{\mu - \rho \left(\frac{k_\gamma}{\omega}\right)^2} . \tag{A-20}$$